Bioresource Technology 102 (2011) 11027–11033

Contents lists available at SciVerse ScienceDirect

Bioresource Technology

journal homepage: www.elsevier.com/locate/biortech

Catalytic pyrolysis of tobacco rob: Kinetic study and fuel gas produced

Yi Yang [a,*], Tan Li [a], Shiping Jin [a], Yixin Lin [a], Haiping Yang [a,b]

[a] School of Energy and Power Engineering, Huazhong University of Science and Technology, Wuhan 430074, PR China
[b] State Key Laboratory of Coal Combustion, Huazhong University of Science and Technology, Wuhan 430074, PR China

ARTICLE INFO

Article history:
Received 11 July 2011
Received in revised form 14 September 2011
Accepted 15 September 2011
Available online 20 September 2011

Keywords:
Catalytic pyrolysis
Kinetic
Tobacco rob
Fuel gas

ABSTRACT

The pyrolysis kinetics of tobacco rob (TR) was investigated using thermogravimetric analysis (TGA) under inert atmosphere, adding chemicals (dolomite and NiO) as catalysts by catalytic-mixing method. The TGA results showed that mass loss and mass loss rates were affected by catalysts. The conversion rates increased while the activation energy decreased. Moreover, the thermal decomposition behaviors of TR were studied in the fixed-bed reactor using dolomite and NiO/γ-Al_2O_3 as catalysts by catalyst-bed method. A series of experiments had been performed to explore the effects of catalysts, and reaction temperature on the composition and yield of fuel gas. The experiments demonstrated that the catalysts had a high activity of cracking tar and hydrocarbons, as well as yielding a high fuel gas production. For both methods, dolomite and NiO revealed better catalytic performance as a view of enhancing conversion rates and increasing product gas yield.

1. Introduction

The bioenergy from biomass was recognized as a potential renewable energy provided for the shortage of the oil (Park et al., 2009). A significant way to obtain the bioenergy was using biomass wastes such as wheat straw, sewage sludge and oil-palm empty fruit bunch (Budarin et al., 2009; Thipkhunthod et al., 2007), because of low cost, extensive source and pollution reduction (Tu et al., 2009). Tobacco plants were widely cultivated in China as an important cigarette material. The tobacco production was 500–550 million tons in China each year. However, tobacco rob (TR) accounted for more than 60% of the total tobacco plants production which could not be used for cigarette production, and the cost was great to deal with them. Thus, TR was often treated by burning as agricultural wastes. It led to serious environmental problems and enormous waste of resources. So, the reutilization of this waste and the exploitation for potential bioenergy would be indispensable.

Biomass thermochemical process including pyrolysis, gasification and combustion was an advanced technology for bioenergy conversion (Cao et al., 2006; Dare et al., 2001; Xiao et al., 2010). For the most applications, the gas should be cleaned to reduce the content of dust and tar (Narváez et al., 1997). The tar formed during biomass pyrolysis was one of the major issues, since catalytic pyrolysis or gasification for tar reduction had been extensively reported in the literatures (Li et al., 2008a,b; Iaquaniello and Mangiapane, 2006). The use of dolomite or nickel oxide as catalysts in biomass pyrolysis or gasification had been attracted much attention, because it was inexpensive and abundant and it could significantly reduce the tar content of the product gas (Hu et al., 2006). Likewise, during TR fast pyrolysis process, dolomite and NiO/γ-Al_2O_3 catalyst were used to eliminate tar. In recent years, the authors had presented a lot of results on the catalytic and non-catalytic pyrolysis of straws, crops, stalks, and municipal solid waste (MSW). But few literatures have been found on catalytic pyrolysis of tobacco rob. Thus this study primarily focused on these feedstocks and their experimental results.

Moreover, a kinetic analysis was performed for better understandings of pyrolysis characteristics and reaction mechanisms during the pyrolysis of tobacco rob. The thermogravimetric data were interpreted by the Doyle fitting method in this study, which allowed the kinetic parameters to be estimated iteratively by linear regression and thus enhances the accuracy (Binlin et al., 2009).

2. Methods

2.1. Samples

The tobacco rob (TR) samples were collected from tobacco waste which was from farm in Enshi City, Hubei Province, China. The samples were dried under the sun for a period of 7 days to reduce the moisture content and then were shredded into particles of sizes of approximately 75 μm. The proximate and ultimate analyses and the heating value of the sample were listed in Table 1.

Two types of pure chemicals, including dolomite and NiO were introduced in TGA as catalysts. Meanwhile, dolomite and NiO/γ-Al_2O_3 were used as catalysts in the fixed-bed reactor. Natural dolomite was ground and sieved with an average diameter of

* Corresponding author. Tel./fax: +86 027 87559603.
E-mail address: yangyi7231@yahoo.com.cn (Y. Yang).

0960-8524/$ - see front matter © 2011 Elsevier Ltd. All rights reserved.
doi:10.1016/j.biortech.2011.09.053

Table 1
Ultimate analysis and proximate analysis of TR.

Ultimate analysis (wt.%)		Proximate analysis (wt.%)	
C	43.33	Moisture content	10.82
H	6.596	Volatile matter	68.34
O[a]	36.86	Fixed carbon	19.30
N	0.758	Ash	1.54
S	0.096	Low heating value (MJ/kg)	20.67

[a] By difference.

5–8 mm. CaO, MgO, SiO_2, Fe_2O_3, Al_2O_3, and LOI contents of dolomite were found to be 30.50%, 20.20%, 2.21%, 0.54%, 0.97% and 45.00%, respectively. The BET surface areas were measured using ASAP2010 with liquid N_2 at 77 K. It was found that dolomite contain very low surface area (0.31 m^2/g). The pore volume of dolomite are 0.07 ml/g. NiO/γ-Al_2O_3 catalyst was prepared using the aqueous solution of $Ni(NO_3)_2{\cdot}6H_2O$ (SCRC, Shanghai) and $CO(NH_2)_2$ (SCRC, Shanghai) and porous γ-Al_2O_3 support substrates in a diameter of ~3 mm (S_{BET} = 120.2 m^2/g, SCRC, Shanghai) by deposition–precipitation (DP) method described in our previous study (Li et al., 2008a,b). The loading amount of NiO was ~10 wt.%. The surface area, pore volume and average pore diameter were 108.5 m^2/g, 0.341 ml/g and 12.2 nm, respectively.

2.2. Thermogravimetric and ultimate analyses

Thermogravimetric analysis of the TR sample and TR-catalyst mixtures were carried out by TA Instrument system (Diamond TG/DTA, PerkinElmer Instruments). Dolomite and NiO and their mixture (1:1) were introduced in TGA as catalyst. The TR sample mass of 5 mg was used for the thermogravimetric analysis without catalysts in the experiment. In the presence of catalyst, the total sample mass was 10 mg. therefore, the mass ratio of TR and catalyst was 1:1. Nitrogen was used as a carrier gas (flow rate 100 ml/min). The heating rate was controlled at 20 °C/min from 20 to 900 °C. All experiments were run in duplicates. Ultimate analysis of the TR sample was obtained with a CHNS/O analyzer (Vario Micro cube, Elementar). Such analysis gave the weight percent of carbon, hydrogen, nitrogen, and sulfur in the sample simultaneously, and the weight percent of oxygen was determined by difference.

2.3. Apparatus and procedures of catalytic pyrolysis

The pyrolysis experiments were conducted at atmospheric pressure, and the apparatus was shown schematically in Fig. 1. The pyrolysis furnace was a quartz tube reactor, with an inner diameter of 60 mm and length of 1200 mm. Prior to each test, catalysts were held in the stainless tube which was sealed by porous ceramic of 59 mm in diameter and 5 mm in thickness. In this case, pyrolytic vapors could pass though the catalyst-bed method which was held at the pyrolysis temperature. The reactor was put inside an electrical furnace, which provided the heat for reactions.

The procedure of experiments is described below. For each test, 2.0 g tobacco rob was put into a porcelain boat which was placed into the quartz tubular reactor when desired temperatures were achieved. The type K thermocouple was used to measure the temperature profile in the middle of the reactor. The temperature controller and electric furnace heater were then turned onto heat the reactor to desired temperature. Nitrogen gas (flow rate of 100 ml/min) was introduced for 40 min to keep anoxic atmosphere and kept constant during experiment. Then porcelain boat was fed into reactor zone simultaneously when the temperature reached desired one. The experiment stopped 5 min later, and the porcelain boat was removed and weighted to determine the amount of unconverted char by difference. The fluid products flowed out the reactor and passed through a water condenser. After every experiment, condensable gas changed into bio-oil was captured by tar collector, while non-condensable gas was collected by a gas-collecting bag for sampling after cleaning. The main gaseous products of H_2, CH_4, N_2, CO, CO_2, C_2H_4 and C_2H_6 were analyzed by GC 9800T with a thermal conductivity detector (TCD). The columns used were TDX-01 for the analysis of H_2, CH_4, CO, CO_2 and 5A, porapak Q for the analysis of C_2H_4, C_2H_6.

The tests mentioned above were performed at five different temperatures: 600, 700, 750, 800 and 850 °C, while dolomite and NiO/γ-Al_2O_3 and their mixture (1:1) were used in the tests and compared with non-catalyst. In this study, each experiment was repeated at least three times to ensure data reliability. The data reported in this study are average value of three times, and data variability was within 5%.

2.4. Methods of data processing

The lower heating value (LHV) of fuel gas was defined as (Mun et al., 2010),

$$\mathrm{LHV\,(kJ/N\,m^3)} = (\mathrm{CO}\times 126.36 + \mathrm{H_2}\times 107.98 + \mathrm{CH_4}\times 358.18 + \mathrm{C_2H_4}\times 590.36 + \mathrm{C_2H_6}\times 637.72) \quad (1)$$

where CO, H_2, CH_4, C_2H_4 and C_2H_6 were the molar percentages of components of the product gas.

3. Results and discussion

3.1. Pyrolysis kinetics

3.1.1. Pyrolysis at different catalysts

From Figs. 2 and 3, the TG and DTG curves of TR pyrolysis and catalytic pyrolysis using different catalysts showed that the small change of conversion in the samples was attributed to vaporization of moisture that was attached on the surface of the samples at the temperature lower than 150 °C, and one major mass loss step occurred between 220 and 360 °C. Meanwhile, the DTG curve had one over-lapping peak and a flat tailing section, and the maximum weight loss rate at different catalysts occurred at about 360 °C. The result was similar to other Chinese biomasses such as rice straw, cotton straw and maize straw reported by Hu et al. (2007). Recently, Thangalazhy-Gopakumar et al. (2011) had re-

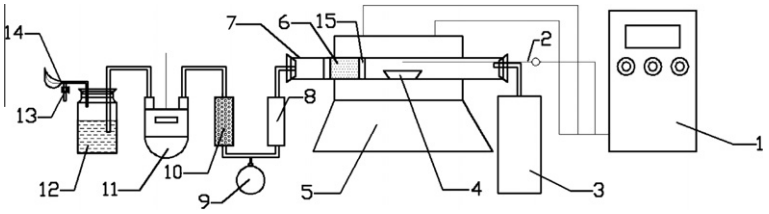

Fig. 1. Experimental apparatus. (1) Temperature controller; (2) thermocouple; (3) nitrogen gas tank; (4) porcelain boat; (5) electric furnace; (6) catalyst; (7) quartz tube reactor; (8) condenser; (9) tar collector; (10) filter; (11) flow meter; (12) water sealed bottle; (13) to gas collector bag; (14) exhaust gas burner; (15) porous ceramic.

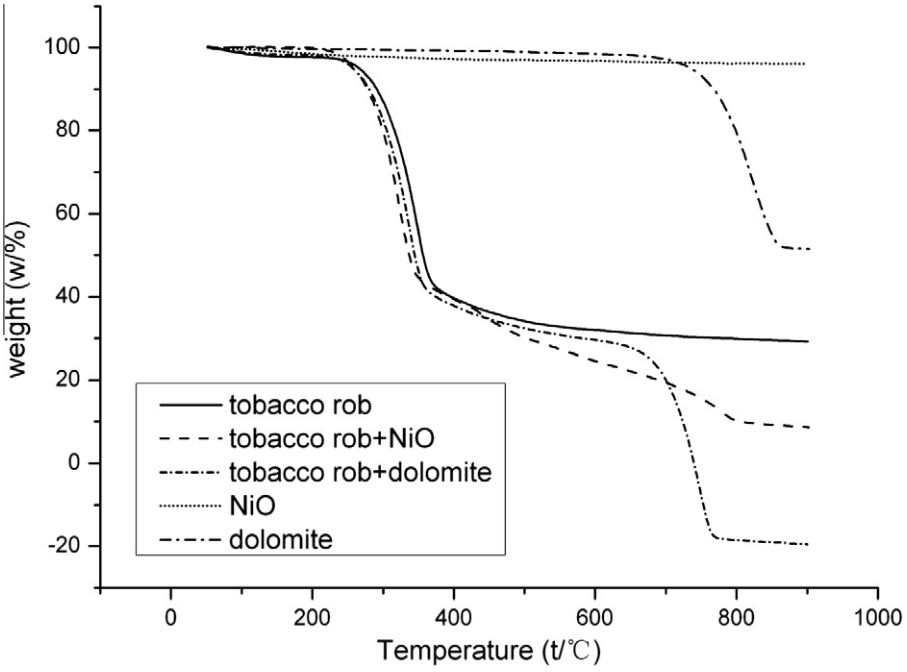

Fig. 2. TG curves of TR catalytic pyrolysis at a heating rate of 20 °C/min.

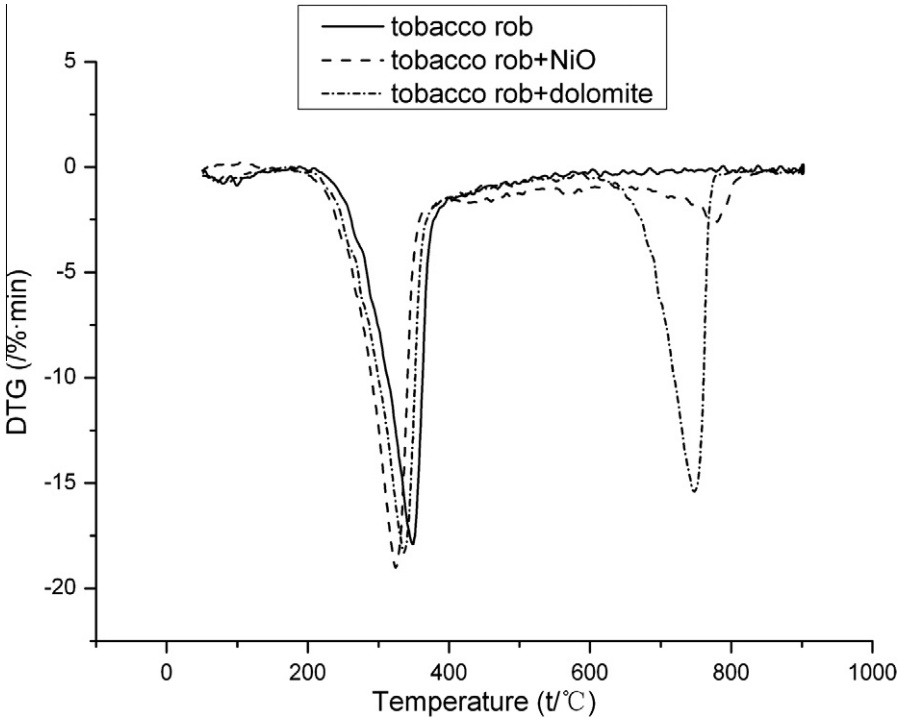

Fig. 3. DTG curves of TR catalytic pyrolysis at a heating rate of 20 °C/min.

ported that a rapid thermal degradation process for pine wood was in the temperature range of 250–400 °C, peaking at around 370 °C. Since the samples contained mainly cellulose, hemicellulose and lignin, it was known that these compositions significantly influenced the biomass pyrolysis process (Sonobe and Worasuwannarak, 2008). Under a slow heating regime, the cellulose was found to decompose between 325 and 375 °C and hemicellulose started to decompose at around 200–300 °C. Lignin had a broad decomposition temperature range at temperatures higher than 280–500 °C (Aguiar et al., 2008; Brito et al., 2008; Shen et al., 2010). So the shoulder peak at lower temperature was attributed to the thermally labile hemicellulose, and the maximum peak represented the decomposition of the cellulose (Fisher et al., 2003; Müller-Hagedorn et al., 2003).

It was observed at temperature below 400 °C that the TG curves shifted slightly to the left in the presence of catalysts and the DTG curves presented that adding catalysts tended to slightly promote thermal degradation processes towards lower temperature. With

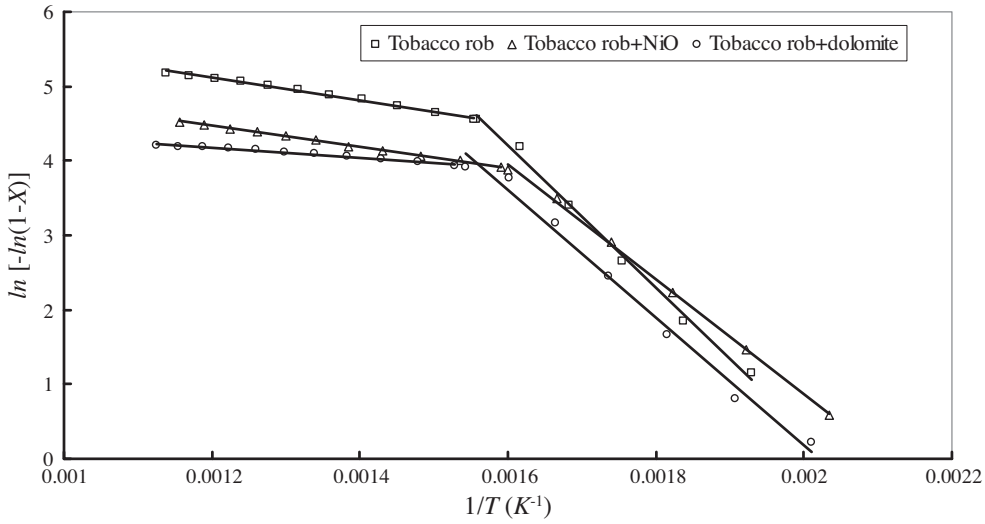

Fig. 4. Relationship between $\ln[-\ln(1-X)]$ and $1/T$ with different catalysts.

the addition of catalysts, the maximum rate of mass loss also increased from 17.86%/min to 19.15%/min and reducing the temperature required to a given percentage conversion by approximately 20–40 °C. These results suggested that the existence of catalysts could decrease the pyrolysis temperature and enhance the gas yield. From Fig. 2, it was clear that the TG curve of TR + dolomite samples showed the second major weight loss stage between 600 and 750 °C, meanwhile the major mass loss stage of dolomite samples appeared at the same temperature range. This showed that the second peak on the DTG curve of TR + dolomite should be caused by the decomposition of dolomite (Zhang et al., 2009). From Fig. 3, the DTG curve of TR + NiO showed an additional peak between 700 and 850 °C. According to the literature data, this additional peak could be attributed to the reduction of the Ni^{n+} species to metallic Ni by amorphous carbon atoms that had been reported to occur at higher temperature (Silva et al., 1997; Koltypin et al., 1999). In the 700–800 °C range, thermodynamic calculations through Ellingham diagrams suggested that nickel oxide reduction could be attributed to the reaction (2) involving the formation of CO (Devi and Kannan, 2007):

$$NiO + C \rightarrow Ni + CO \quad (2)$$

For further investigation, the TG and DTG curves of TR pyrolysis using mixture of dolomite and NiO as mixed catalyst are shown in Fig. 6. The initial weight loss until 150 °C can be contributed to the loss of moisture in the sample under inert atmosphere. It was clear that a rapid thermal degradation was noticed for TR in the temperature range of 250–350 °C, peaking at around 320 °C. Moreover, the maximum rate of mass loss of TR was more significant with mixed catalyst (18.87%/min) than without catalyst (17.86%/min). The reason may be that some volatile compounds might have been produced in the presence of the mixed catalyst. Nonetheless, from Fig. 6, the DTG curve showed two additional peaks between 400 and 600 °C. They could be attributed to the reduction of NiO to nickel by carbon and the decomposition of dolomite as the tests mentioned above (Devi and Kannan, 2007; Zhang et al., 2009).

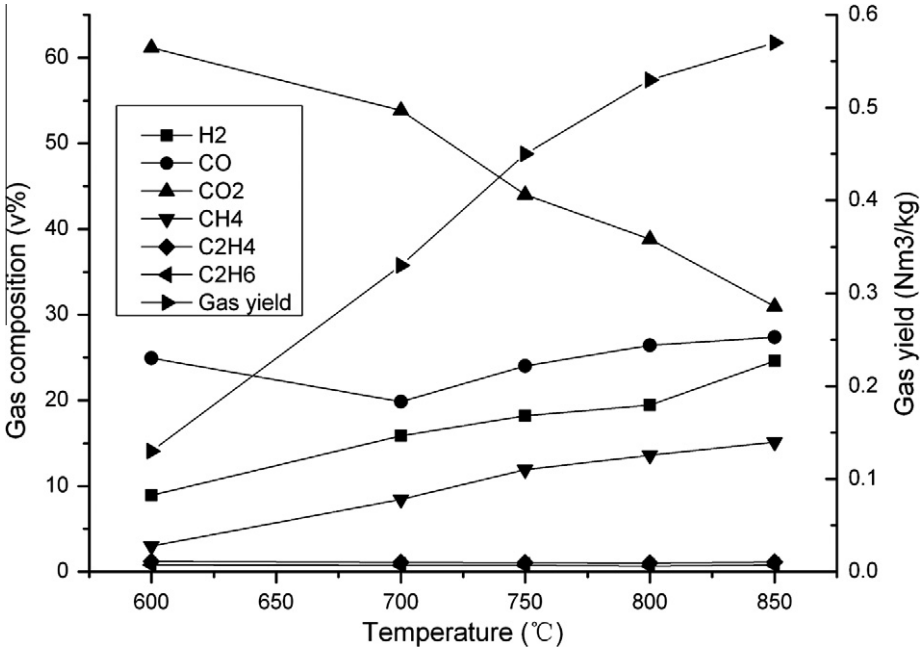

Fig. 5. Effect of temperature on gas yield and gas composition in TR pyrolysis for non-catalytic process.

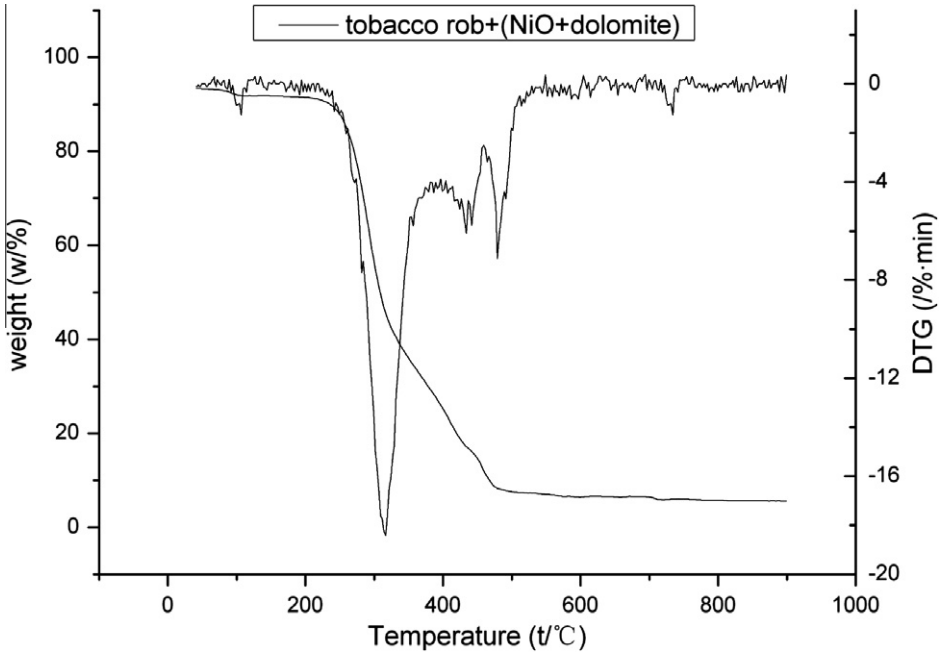

Fig. 6. Pyrolysis curves of TR with mixed catalyst in TGA.

3.1.2. Kinetics parameters

There were so many researches on the kinetics of pyrolysis of biomass, and various mechanisms and assumptions were illustrated. In this work, the kinetic parameters for the pyrolysis process of TR could be calculated using similar procedure adopted by Xiao et al. (2007).

The results of thermogravimetric experiments were expressed as conversion X, defined as:

$$X = (W_0 - W_t)/(W_0 - W_f) \quad (3)$$

where W_0, W_t and W_f were the initial mass of the sample, the mass of pyrolysis sample, and the final residual mass, respectively.

The general non-isothermal, decomposition reaction rate was:

$$dX/dt = k(1 - X)^n \quad (4)$$

The reaction rate constant k was expressed by the Arrhenius equation

$$k = A\exp(-E/RT) \quad (5)$$

T was the temperature, A was the pre-exponential factor, t was the time, E was the activation energy, R was the universal gas constant (8.314 J/kmol), n was the reaction order, β was the heating rate. In many applications, the pyrolysis of biomass was assumed to be a first-order reaction (i.e., $n = 1$). Eq. (4) could be rearranged to:

$$\frac{dX}{dT} = \frac{A}{\beta}\cdot\exp\left(-\frac{E}{RT}\right)\cdot(1 - X) \quad (6)$$

Assuming that the catalytic pyrolysis of biomass followed apparent first-order reaction kinetics, the Doyle integral method was used to analyze the pyrolytic characters of this complicated process. The Doyle formula used to calculate the kinetic parameters of first-order reaction was as follows:

$$\ln[-\ln(1 - X)] = \ln\frac{AR}{\beta E} - 5.3308 - 1.0516\frac{E}{RT} \quad (7)$$

Using the 20 °C/min reaction as an example, the relationship between $\ln[-\ln(1 - X)]$ and $1/T$ under different catalytic pyrolysis situation was shown in Fig. 4.

Table 2
Activation energy based on Doyle calculation.

	Temperature (°C)	Conversion (%)	E (kJ/mol)	R^2
TR	248–373	5.9–83	78.39	0.9959
	373–875	83–99.6	11.62	0.9932
TR + NiO	219–356	4.0–60	62.28	0.9957
	356–734	60–90	11.50	0.9959
TR + dolomite	224–381	5.0–61	70.03	0.9917
	381–667	61–74	5.20	0.9889
TR + mixed catalyst	230–320	11.2–60	69.48	0.9919
	320–698	60–90.1	24.4	0.9910

The slopes and intercepts of the $\ln[-\ln(1 - X)]$ versus $1/T$ curves were used to calculate the kinetic parameters when each curve was divided into two sections, according to its linearity characteristics. The calculated kinetic parameters were listed in Table 2.

In the TGA results, several data were selected to satisfy a best linear regression of Eq. (7). All the regression results had nearly extreme coefficients of determination, R^2 (from 0.9889 to 0.9959). Therefore, the assumption that pyrolysis of biomass underwent a first-order reaction should be proper. From Fig. 4 and Table 2, it can be seen that both biomass pyrolysis and catalytic pyrolysis exhibited typical, multi-step reaction characteristics. In the first-step reaction, the activation energy ranged from 62.28 to 78.39 kJ/mol for TR pyrolysis and catalytic pyrolysis. The apparent activation energy for the catalytic pyrolysis is lower than that for non-catalytic pyrolysis. The catalysts significantly increased the rate of reaction, reducing the temperature required to a given percentage conversion by approximately 20–40 °C. During the second-step reaction, the activation energy for TR pyrolysis was 11.62 kJ/mol, and the value changed to 11.50 and 5.20 kJ/mol with NiO and dolomite, respectively. Nevertheless, in this step, the mixed catalyst demonstrated the highest activation energy. This shows that the mixed catalyst had some influence in thermal decomposition at a lower temperature although there might be less influence at a higher temperature. Dolomite appeared a stronger effect on the TR pyrolysis process than NiO. For these steps, the turning points of conversion dropped from about 83 wt.% for biomass

Table 3
Results of TR pyrolysis with different catalysts at 850 °C.

Catalyst	Components of the gas product (vol.%)						Gas yield (N m^3/kg)	LHV (M J/m^3)
	H_2	CO	CH_4	CO_2	C_2H_4	C_2H_6		
No catalyst	24.63	27.37	13.15	32.95	1.12	0.78	0.57	11.99
NiO/γ-Al_2O_3	38.96	31.85	16.91	12.01	0.18	0.09	1.06	14.45
Dolomite	30.06	28.81	19.93	20.29	0.12	0.11	0.93	14.24
Mixed catalyst	37.25	32.13	15.88	14.47	0.17	0.10	0.98	13.93

pyrolysis to 60 wt.% for biomass catalytic pyrolysis. According to the literature data, similar results were studied by Lu et al. (2009).

3.2. Fuel gas produced in a fixed-bed reactor

3.2.1. Effect of reaction temperature

Biomass pyrolysis reaction could be divided into two steps (Dai et al., 2000). The first step was a thermo-chemical decomposition of TR with production of tar, char and volatiles. This step termed primary pyrolysis, performed at a lower temperature ~300 °C, and lasted until a temperature of 700 °C or even higher. The second step was followed by tar cracking of and conversion. This step ought to occur at higher temperatures (>400 °C). The main secondary reactions of oil cracking and shifting include decarboxylation, dehydrogenation, cyclization, aromatization, and polymerizing reactions, which were given in order of increasing pyrolysis severity (e.g., increasing temperature). In the present study, the micro-pyrolyzer setup used to distinguish and determine the extent of secondary reactions was reported by Patwardhan et al. (2011).

The gas species distribution profiles from TR pyrolysis at different final temperatures are plotted in Fig. 5. The H_2 content increased steadily from 8.93% to 24.63% as the temperature increased from 600 to 850 °C. Yields of CH_4 also increased from 2.98% to 13.15%, while CO_2 content decreased in general with increasing temperature. The yield of CO decreased first from 24.94% to 19.88% as the temperature increased to 700 °C, then it increased again to 27.37% as the temperature continuously increased to 850 °C. The yields of C_2H_4 and C_2H_6 were relatively small, and the influence of temperature was insignificant. Overall, H_2 and CH_4 contents increased sharply with the increase of the reactor temperature, while CO_2, C_2H_4 and C_2H_6 contents exhibited the opposite tendencies. Thus, the reaction temperature was an important factor with regard to final composition of the gases.

3.2.2. Effect of catalyst

According to the literatures (Florin and Harris, 2008; Li et al., 2008a,b; Yang et al., 2007), catalysts are expected to influence product gas quantity and composition in two main ways: (i) improving tar cracking reactions by catalyzing C–C bond cleavage; (ii) enhancing the reforming of light gas molecules, e.g., breaking C–H bonds. The main gas-phase reactions were shown as:

$$\text{Biomass} \rightarrow H_2O + H_2 + CO + CO_2 + \text{volatiles} + \text{tars} + \text{char(Pyrolysis)} \quad (8)$$

$$\text{Tars} \rightarrow H_2O + H_2 + CO + CO_2 + CH_4 + CxHy + C_2H_5OH + CH_3OH + CH_2O + CH_3CHO \quad \text{(Tars cracking(catalytic))} \quad (9)$$

$$C_2H_5OH \rightarrow CH_3CHO + H_2 \quad \text{(Catalytic cracking)} \quad (10)$$

$$CH_3CHO \rightarrow CH_4 + CO \quad \text{(Catalytic cracking)} \quad (11)$$

$$CH_2O \rightarrow CO + H_2 \quad \text{(Catalytic cracking)} \quad (12)$$

The results of catalytic pyrolysis of TR at 850 °C are listed in Table 3. It can be seen that when the volatiles were passed through the catalytic bed with the supported NiO/γ-Al_2O_3 catalyst and dolomite at 850 °C. There were the marked increases in gas yield and LHV. With the addition of NiO/γ-Al_2O_3, gas yield and LHV drastically increased from 0.57 to 1.06 N m^3/kg and 11.99 M J/m^3 to 14.45 M J/m^3, respectively. Meanwhile, in the presence of dolomite, gas yield and LHV reached 0.93 N m^3/kg and 14.25 M J/m^3, respectively. This indicated that the catalysts had a highly positive performance for fuel gas production and tar reduction in biomass pyrolysis. The significant increase in gas yield was due to predominantly the secondary cracking occurred on the surface of the catalysts. The similar finding on other biomass materials for pyrolysis was also reported by Devi et al. (2005) and Garcia et al. (2001).

As for the individual gas, in the presence of catalysts, H_2, CO and CH_4 contents increased drastically, while CO_2, C_2H_4 and C_2H_6 contents showed the opposite tendencies. From these changes of gas composition, it could be concluded that several reactions (Eqs. (9)-(12)) occurred probably in the catalytic reactor (Zhao et al., 2010). The highest H_2 and CO contents were obtained with NiO/γ-Al_2O_3 catalyst. In contrast, with regards to CH_4 production, the highest content (19.93%) was found with dolomite. These results showed that the presence of catalysts could induce the equilibrium for the several reactions (Eqs. (10)-(12)) to be shifted towards H_2, CO and CH_4 production.

Moreover, for further investigation, the catalytic activity of mixed catalyst was determined by catalyst-bed method in fixed-bed reactor at 850 °C. To compare the activities of catalysts, the contents of different gas components and fuel gas yield that evolved with mixed catalyst are plotted in Table 3. It indicates that the mixed catalyst has high catalytic activity and the difference between the activities of mixed catalyst and NiO/γ-Al_2O_3 is quite small. Therefore, NiO played a dominant role in the catalytic activity of mixed catalyst. Overall, the catalysts enhanced markedly the cracking of tar and of large molecular hydrocarbons in gaseous products to generate valuable fuel gas.

4. Conclusions

Pyrolytic behaviors of TR and TR-catalyst mixtures (1:1) were studied in TGA. Decreasing temperature for the primary decomposition of TR was attributed to adding catalysts. The fuel gas produced from TR catalytic pyrolysis in the fixed-bed reactor was also studied by catalyst-bed method. The results indicated that the presence of catalysts influenced greatly the product gas yield and gas composition in pyrolysis process. Meanwhile, higher temperature resulted in higher yield of fuel gas and higher LHV. It was proven that TR could be considered as a waste material for useful and valuable fuel gas.

Acknowledgements

This research was supported by the National Natural Science Foundation of China (No. 51076057). The authors are grateful to the Analytical and Testing Center of State Key Laboratory of Coal Combustion for carrying out the ultimate analysis and the thermogravimetric analysis of the samples.

References

Aguiar, L., Márquez-Montesinos, F., Gonzalo, A., Sánchez, J.L., Arauzo, J., 2008. Influence of temperature and particle size on the fixed bed pyrolysis of orange peel residues. J. Anal. Appl. Pyrol. 83, 124–130.

Binlin, D., Valerie, D., Paul, T.W., Chen, H.S., Ding, Y.L., 2009. Thermogravimetric kinetics of crude glycerol. Bioresour. Technol. 100, 2613–2620.
Brito, J.O., Silva, F.G., Leao, M.M., Almeida, G., 2008. Chemical composition changes in eucalyptus and pinus woods submitted to heat treatment. Bioresour. Technol. 99, 8545–8548.
Budarin, V.L., Clark, J.H., Lanigan, B.A., Shuttleworth, P., Breeden, S.W., Wilson, A.J., Macquarrie, D.J., Milkowski, K., Jones, J., Bridgeman, T., Ross, A., 2009. The preparation of high-grade bio-oils through the controlled, low temperature microwave activation of wheat straw. Bioresour. Technol. 100, 6064–6068.
Cao, Y., Wang, Y., Riley, J.T., Pan, W.P., 2006. A novel biomass air gasification process for producing tar-free higher heating value fuel gas. Fuel process. Technol. 87, 343–353.
Dare, P., Gifford, J., Hooper, R.J., Clemens, A.H., Damiano, L.F., Gong, D., Matheson, T.W., 2001. Combustion performance of biomass residue and purpose grown species. Biomass Bioenergy 21, 277–287.
Dai, X., Wu, C., Li, H.B., Chen, Y., 2000. The fast pyrolysis of biomass in CFB reactor. Energy Fuels 14 (3), 552–557.
Devi, L., Ptasinski, K.J., Janssen, F.J.J.G., van Paasen, S.V.B., Bergman, P.C.A., Kiel, J.H.A., 2005. Catalytic decomposition of biomass tars: use of dolomite and untreated olivine. Renewable Energy 30, 565–587.
Devi, T.G., Kannan, M.P., 2007. X-ray diffraction (XRD) studies on the chemical states of some metal species in cellulosic chars and the Ellingham diagrams. Energy Fuels 21, 596–601.
Fisher, T., Hajaligol, M., Waymack, B., Kellogg, D., 2003. Pyrolysis behavior and kinetics of biomass derived materials. J. Anal. Appl. Pyrol. 62, 331–349.
Florin, N.H., Harris, A.T., 2008. Mechanistic study of enhance H_2 synthesis in biomass gasifiers with insitu CO_2 capture using CaO. AIChE J. 54, 1096–1109.
Garcia, L., Salvador, M.L., Arauzo, J., Bilbao, R., 2001. Catalytic pyrolysis of biomass: influence of the catalyst pretreatment on gas yields. J. Anal. Appl. Pyrol. 58–59, 491–501.
Hu, G., Xu, S.P., Li, C.G., Liu, S.Q., 2006. Steam gasification of apricot stones with olivine and dolomite as downstream catalysts. Fuel. process. Technol. 87, 375–382.
Hu, S., Jess, A., Xu, M.H., 2007. Kinetic study of Chinese biomass slow pyrolysis: comparison of different kinetic models. Fuel 86, 2778–2788.
Iaquaniello, G., Mangiapane, A., 2006. Integration of biomass gasification with MCFC. Int. J. Hydrogen Energy 31, 399–404.
Koltypin, Y., Fernandez, A., Rojas, T.C., Campore, J., Palma, P., Prozorov, R., Gedonken, A., 1999. Encapsulation of nickel nanoparticles in carbon obtained by the sonochemical decomposition of $Ni(C_8H_{12})$. Chem. Mater. 11, 1331–1335.
Li, J.F., Yan, R., Xiao, B., Liang, D.T., Du, L.J., 2008a. Development of nano-NiO/Al_2O_3 catalyst to be used for tar removal in biomass gasification. Environ. Sci. Technol. 42, 6224–6229.
Li, J.F., Yan, R., Xiao, B., Liang, D.T., Lee, D.H., 2008b. Preparation of nano-NiO particles and evaluation of their catalytic activity in pyrolyzing biomass components. Energy Fuels 22, 16–23.
Lu, C.B., Song, W.L., Lin, W.G., 2009. Kinetics of biomass catalytic pyrolysis. Biotechnol. Adv. 27, 583–587.
Müller-Hagedorn, M., Bockhorn, H., Krebs, L., Müller, U., 2003. A comparative kinetic study on the pyrolysis of three different wood species. J. Anal. Appl. Pyrol. 68–69, 231–249.
Mun, T.Y., Seon, P.G., Kim, J.S., 2010. Production of a producer gas from woody waste via air gasification using activated carbon and a two-stage gasifier and characterization of tar. Fuel 89, 3226–3234.
Narváez, I., Corella, J., Orio, A., 1997. Fresh tar (from a biomass gasifier) elimination over a commercial steam reforming catalyst. Kinetics and effect of different variables of operation. Ind. Eng. Chem. Res. 36, 317–327.
Park, Y.H., Kim, J.S., Kim, S.S., Park, Y.K., 2009. Pyrolysis characteristics and kinetics of oak trees using thermogravimetric analyzer and micro-tubing reactor. Bioresour. Technol. 100, 400–405.
Patwardhan, P.R., Dalluge, D.L., Shanks, B.H., Brown, R.C., 2011. Distinguishing primary and secondary reactions of cellulose pyrolysis. Bioresour. Technol. 102, 5265–5269.
Shen, D.K., Gu, S., Luo, K.H., Wang, S.R., Fang, M.X., 2010. The pyrolytic degradation of wood-derived lignin from pulping process. Bioresour. Technol. 101, 6136–6146.
Silva, I.F., Mckee, D.W., Lobo, L.S., 1997. A kinetic and in situ XRD study of carbon reactions catalyzed by nickel, cobalt, molybdenum, and their mixtures. J. Catal. 170, 54–61.
Sonobe, T., Worasuwannarak, N., 2008. Kinetic analyses of biomass pyrolysis using the distributed activation energy model. Fuel 87, 414–421.
Thangalazhy-Gopakumar, S., Adhikari, S., Gupta, R.B., Tu, M.B., Taylor, S., 2011. Production of hydrocarbon fuels from biomass using catalytic pyrolysis under helium and hydrogen environments. Bioresour. Technol. 102, 6742–6749.
Thipkhunthod, P., Meeyoo, V., Rangsunvigit, P., Rirksomboon, T., 2007. Describing sewage sludge pyrolysis kinetics by a combination of biomass fractions decomposition. J. Anal. Appl. Pyrol. 79, 78–85.
Tu, W.K., Shie, J.L., Chang, C.Y., Chang, C.F., Lin, C.F., Yang, S.Y., Kuo, J.T., Shaw, D.G., You, Y.D., Lee, D.J., 2009. Products and bioenergy from the pyrolysis of rice straw via radio frequency plasma and its kinetics. Bioresour. Technol. 100, 2052–2061.
Xiao, R.R., Chen, X.L., Wang, F.C., Yu, G.S., 2010. Pyrolysis pretreatment of biomass for entrained-flow gasification. Appl. Energy 87, 149–155.
Xiao, J., Shen, L.H., Zheng, M., Wang, Z.M., Zhong, X.L., 2007. TG-FTIR study on catalytic pyrolysis of biomass (in Chinese). J. Fuel Chem. Technol. 35 (3), 215–220.
Yang, H.P., Yan, R., Chen, H.P., Lee, D.H., Zheng, C.G., 2007. Characteristics of hemicellulose, cellulose and lignin pyrolysis. Fuel 86, 1781–1788.
Zhang, S.Y., Hong, R.Y., Cao, J.P., Takayuki, T., 2009. Influence of manure types and pyrolysis conditions on the oxidatation behavior of manure char. Bioresour. Technol. 100, 4278–4283.
Zhao, B.F., Zhang, X.D., Li, S., Meng, G.F., Chen, L., Lu, Y.X., 2010. Hydrogen production from biomass combining pyrolysis and secondary decomposition. Int. J. Hydrogen Energy 35, 2606–2611.